

Astro. Lett. and Communications, 1995, Vol. 32, pp. 217–222
Reprints available directly from the publisher
Photocopying permitted by license only

© 1995 OPA (Overseas Publishers Association)
Amsterdam B.V. Published under license by
Gordon and Breach Science Publishers SA
Printed in Malaysia

1995-02-23
NASA-1082

1995-02-23

A Degree-Scale Measurement of the Anisotropy in the Cosmic Microwave Background

ED WOLLACK, NORM JAROSIK, BARTH NETTERFIELD, LYMAN PAGE
and DAVID WILKINSON *Dept. of Physics, P.O. Box 708, Jadwin Hall,
Princeton University, Princeton, NJ 08544*

(Received 4 February 1994; in final form 30 November 1994)

We report the detection of anisotropy in the microwave sky at 30 GHz and at 1° angular scales. The most economical interpretation of the data is that the fluctuations are intrinsic to the cosmic microwave background. However, galactic free-free emission is ruled out with only 90% confidence. The most likely root-mean-squared amplitude of the fluctuations, assuming they are described by a Gaussian auto-correlation function with a coherence angle of 1.2° , is $41^{+16}_{-13} \mu\text{K}$. We also present limits on the anisotropy of the polarization of the cosmic microwave background.

KEYWORDS: Cosmic microwave background cosmology

THE INSTRUMENT, OBSERVING STRATEGY, AND DATA

The radiometer views the sky in three frequency bands, (26–29, 29–32, and 32–35 GHz) in two polarizations. Radiation from the sky is amplified by low-noise high electron mobility amplifiers (HEMT amplifiers, Pospieszalski *et al.*, 1988, Pospieszalski 1992) and detected with commercial RF diodes. A similar technique was used by Gaier *et al.* (1992). All six channels detect radiation from the sky through a cooled corrugated horn that feeds an off-axis parabolic section. After reflecting off the parabola, the beam has a FWHM of 1.44° . The beam is then directed to different positions on the sky by a 90 cm by 150 cm oscillating plate that rotates in azimuth. The elevation of the beam is fixed at 52.14° , the latitude of the observing site in Saskatoon, Canada. The calibration and pointing are done using Cassiopeia A as a source, with the instrument in the configuration used for anisotropy measurements. A schematic of the instrument is shown in Figure 1; further details are given in Wollack *et al.* (1993). The experiment has been referred to as both BIGPLATE and SK93 in the literature.

The sky is observed by sweeping the beam in a sinusoidal pattern of amplitude 2.45° on the sky (the azimuthal amplitude is $4^\circ = 2.45^\circ/\cos(52.14^\circ)$). The data stream is demodulated at the second harmonic of the chop frequency so that the resulting beam pattern resembles a “double-difference” or “triple-beam-chop.” We use the term “signal” to refer to the value of the demodulated data. The effective window function (for example, Bond, 1992) is approximated by

$$W_l(\sigma, \theta_i) = \{1.5 - 2P_l(\cos \theta_i) + 0.5P_l(\cos 2\theta_i)\} \exp(-l(l+1)\sigma^2) \quad (1)$$

where the Gaussian beamwidth is $\sigma = 0.65^\circ$ ($0.4246 \theta_{\text{FWHM}}$) and the beam throw is $\theta_i = 2.45^\circ$. The center of the pattern is alternated between a point 4.9° west of the north

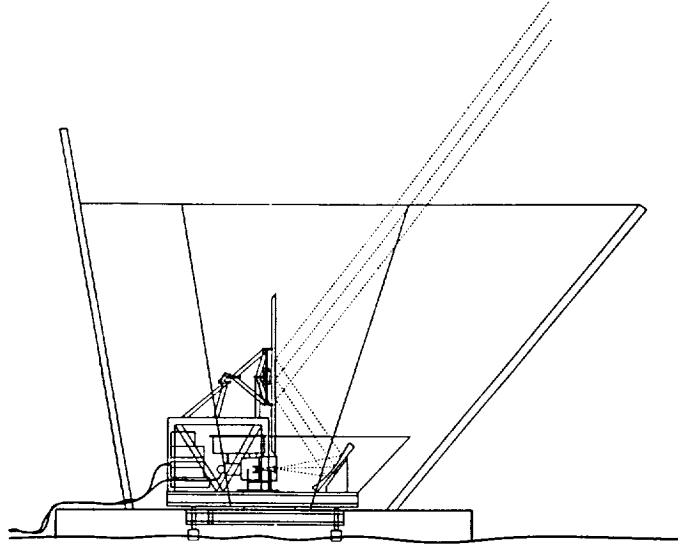


FIGURE 1 Schematic of the instrument. The outermost dashed lines mark the -3 dB level of the beam. The instrument observes both day and night; ground screens shield the instrument from the solar and terrestrial radiation.

celestial pole (NCP) and a point 4.9° east of the NCP with a period of 32.4 s. The east and west data are treated independently. The pattern swept out on the sky is shown in Figure 2. (Note that our coverage overlaps the MSAM coverage (Cheng *et al.*, 1993).

The radiometer is very stable. The mean value of the signal, often called the offset, is less than $400 \mu\text{K}$ in all channels, and depends on the channel and the east/west base position. There were no significant changes in the offset over the three weeks in which data were taken. This makes the analysis fairly straightforward; there is no filtering and no subtraction of a time-varying component. Data from the quadrature demodulation are consistent with zero, indicating that the electronic offset is insignificant. The results of the analysis are shown in Figure 3. For this plot, the data taken while looking east are shifted by 12 h and added to the data taken while looking west. Also, both polarizations are combined. A signal with approximately equal amplitude in each frequency band is evident, though a complete analysis is needed to determine the spectral index, β . In principle, the experiment could have been done with the radiometer held stationary in either the east or west position alone. The east/west wobble provides a second level of modulation. It allows us to discriminate between signals fixed to the sky and those due to systematics linked to day/night or east/west effects.

ANALYSIS

In the microwave regime, sources of radiation may be modeled as $T(f) \propto f^\beta$. Despite the limited frequency range of this experiment, galactic sources with $\beta = -2.1$ (free-free

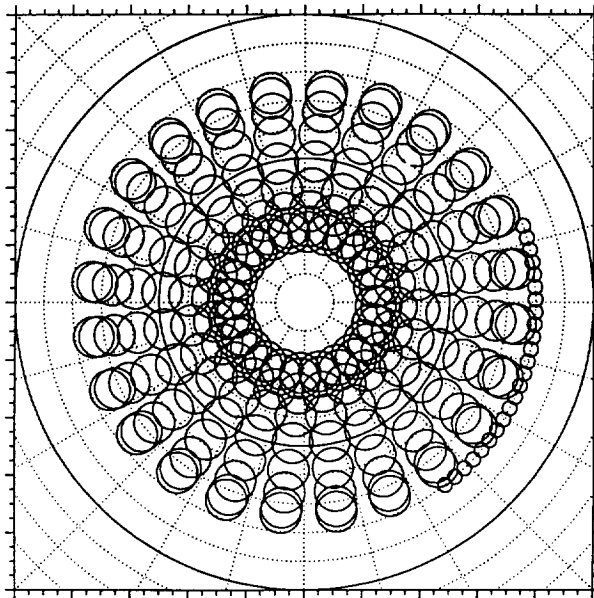


FIGURE 2 Observing pattern for SK93. The north celestial pole is at the center of the figure. The concentric circular dotted lines are 1° increments in declination. The radial lines are 15° increments in right ascension. The instrument chops and wobbles only in the east-west direction and the sky rotates through the beam. The 1.5° diameter circles show approximately where the sky is sampled. The sampling is actually continuous in both right ascension and declination. The small circles near $\delta = 82^\circ$ on the right of the plot indicate the MSAM coverage.

emission) and $\beta = -2.8$ (synchrotron emission) can be differentiated from thermal sources, such as the CMB, with $\beta = 0$. Although much can be learned about possible galactic contributions to the signal by considering lower frequency maps (Haslam, 1982; Reich and Reich, 1986) and catalogs of point sources, we concentrate here on what the data alone tell us.

To find both the best index β and the root-mean-squared amplitude of the signal we model the correlation function as

$$C(\theta, \beta) = (f_1 f_2)^\beta C_0 c(\theta). \quad (2)$$

where f_1 is the frequency of channel 1 and $c(\theta)$ contains all the spatial information about the correlation function. The likelihood of the data is maximized as a function of the two variables and a contour plot is produced (Wollack *et al.*, 1993). In our formulation of the likelihood, we take into account the inherent correlations produced by the atmosphere and the HEMT amplifiers. One effect of these correlations is to increase the error bars over those found from a more native analysis.

To test Gaussian auto-correlation functions (GACFs), the spatial part of the correlation function is set to $c(\theta) = \exp(-\theta^2/2\theta_c^2)$ where $\theta_c = 1.2^\circ$, the correlation angle. Contours of the likelihood are plotted in the $C_0^{1/2} - \beta$ plane in Figure 4. The most

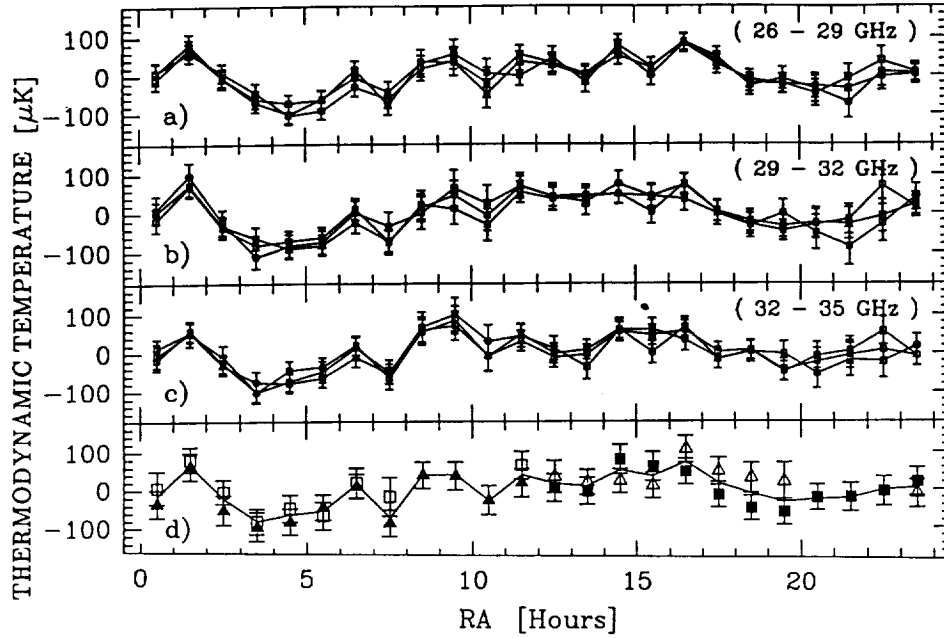


FIGURE 3 The data referenced to the top of the atmosphere. Panels (a), (b) and (c) show data from each of the frequency bands. Data taken while looking west have been shifted 12 h and combined with data taken while looking east. Both polarizations are added together. The three different lines in each panel correspond to three different cut levels for rejecting data due to bad weather. There is clearly a signal present in all channels that is independent of atmospheric cut. In panel (d), the data are separated according to when and where they were taken. The unfilled symbols represent data taken during the day, the filled symbols are for data taken at night. The squares are for data taken while looking east and the triangles for data taken looking west. Note that all combinations of data are consistent.

likely values are $C_0^{1/2} = 41_{-13}^{+16} \mu\text{K}$ and $\beta = -0.3_{-1.2}^{+0.7}$. The errors are determined by integrating the likelihood. Typically, a likelihood of 0.15 corresponds to a 5% (or 95%) confidence limit. The contours are bowed slightly to the negative index side. This may hint at some free-free contamination, but clearly, the contribution is not large.

The current trend in reporting results is to give the rms amplitude of the data along with the window function. This way, theories may easily be related to the data without recourse to the GACF. The square of the rms of the observations is given by

$$\Delta_{\text{rms}}^2 = \frac{1}{4\pi} \sum_{l=2}^{\infty} (2l+1) C_l W_l(\sigma, \theta) \quad (3)$$

where the C_l are the Legendre transform coefficients for any theory and W_l is given in Eq. (1). The model in Eq. (2) may be used to compute Δ_{rms}^2 by setting $c(\theta) = \delta(\theta)$. We find $\Delta_{\text{rms}} = 33 \pm 10 \mu\text{K}$ and $\beta = -0.3_{-1.2}^{+0.7}$. If instead, the Legendre transform of the GACF is used for the C_l in Eq. (3), we find $\Delta_{\text{rms}} = 32 \mu\text{K}$.

Because we have data for two orthogonal polarizations at each frequency, we can also set a limit on the anisotropy in the polarization. We find $\Delta_{\text{rms}}^{\text{pol}} < 25 \mu\text{K}$ with 95%

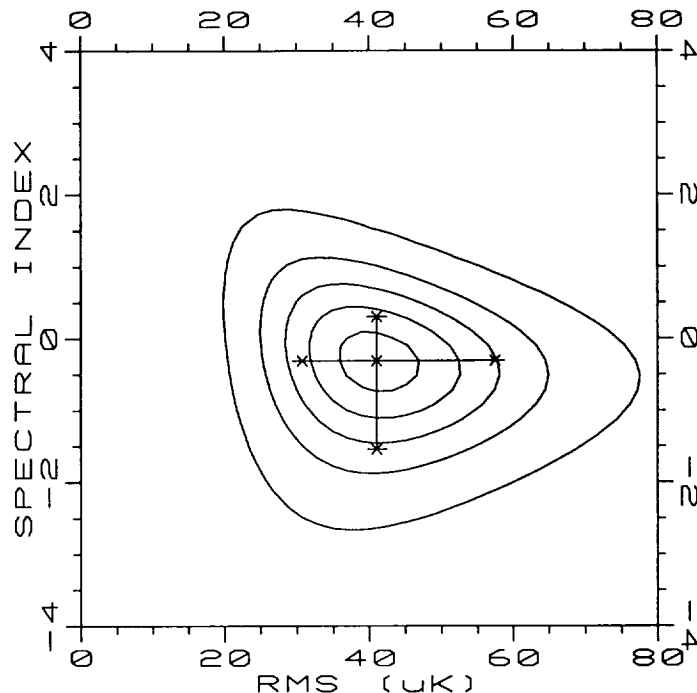


FIGURE 4 Results from the Gaussian auto-correlation function analysis. The y-axis is the spectral index and the x-axis is $C_0^{1/2}$. The values of the likelihood for the contours shown are 0.1, 0.3, 0.5, 0.7, 0.9. The “1 σ ” error bars depict the span between 16% and 84% of the total integrated likelihood and the maximum of the likelihood is at (41 μK , -0.3). This analysis may be directly compared with that of other experiments. Gaier *et al.* (1992) give a 95% confidence upper limit: $C_0^{1/2} \leq 38 \mu\text{K}$. Schuster *et al.* (1993) report a detection of $C_0^{1/2} = 23^{+22}_{-10} \mu\text{K}$ (2 σ error bars) but an index $\beta = -2^{+1.5}_{-1.8}$.

confidence. Note that this also serves as a check for systematics; the difference between signals from orthogonal polarizations at the same frequency is consistent with zero.

If the C_l from “standard CDM” ($h = 0.5$, $\Omega_b = 0.05$, $P(\kappa) \propto \kappa$; Steinhardt, 1993) are used in Eq. (3), then $\Delta_{\text{rms}} = 37 \mu\text{K}$ is predicted, consistent with our results. With the current errors, it is too early to discriminate between the many competing cosmological models at these angular scales. However, given these results and those from other experiments we can now be fairly confident that the anisotropy persists to smaller angular scales than those probed by *COBE*.

ACKNOWLEDGMENTS

This work benefited from many people’s suggestions and labor. In particular, we thank George Sofko and Mike McKibben at the University of Saskatchewan’s Institute for Space and Atmospheric Studies and Larry Snodgrass at the Canadian SRC for valuable assistance with our Saskatoon operations. We also thank Marian Pospieszalski and Mike Balister at NRAO for providing the amazing HEMT amplifiers. This work was supported by NASA grants NAGW-2801 and NAGW-1482, the NSF grant PH89-21378 and a NSF NYI grant to L. Page.

Note added in proof

The findings reported in this paper were confirmed in a subsequent observing campaign. The new results are given in Netterfield *et al.* 1995.

REFERENCES

- Bond, J. R., 1992, Cosmic Structure Formation & The Background Radiation, Proceedings of the IUCAA Dedication Ceremonies, Pune, India, ed. T. Padmanabhan, Wiley. And in: Evolution of Galaxies and Their Environments (Kluwer) 3rd edn. Teton Summer School, ed. M. Shall, H. Thronson, July 1992.
- Cheng, E. S. *et al.*, 1994, *Ap. J.*, **422**, L37.
- Gaier, T. *et al.*, 1992, *Ap. J.*, **398**, L1.
- Haslam, C. G. T., Salter, C. J., Stoffel, H. and Wilson, W. E., 1982, *A&AS*, **47**, 1.
- Netterfield C. B. *et al.*, Submitted to *Ap. J.* 1995.
- Pospieszalski, M., Weinreb, S., Norrod, R. and Harris, R., 1988, *IEEE, MTT*, **36**, 552.
- Pospieszalski, M., 1992, *IEEE, MTT-S*, 1369.
- Reich, P. and Reich, W., 1986, *A&AS*, **63**, 205.
- Schuster, J. *et al.*, 1993, *Ap. J.*, **412**, L47.
- Steinhardt, P. J., 1993, Private communication.
- Wollack, E. *et al.*, 1993, *Ap. J.*, **419**, L49.